Localization Of Narrowband Radio Emitters Based on Doppler Frequency Shifts

Alon Amar* and Anthony J. Weiss§

School of Electrical Engineering - Systems Department

Tel Aviv University, Tel Aviv 69978, Israel

Abstract

Several techniques for emitter localization based on the Doppler effect have been described in the literature. One example is the Differential Doppler method in which the signal of a stationary emitter is intercepted by at least two moving receivers. The frequency difference between the receivers is measured at several locations along their trajectories and the emitter's position is then estimated based on these measurements. This two-step approach is suboptimal since each frequency difference measurement is performed independently, although all measurements correspond to a common emitter position. Instead, a single step approach based on the maximum likelihood criterion is proposed here for both known and unknown waveforms. The position is determined directly from all the observations by a search in the position space. Simulations show that the proposed method outperforms the Differential Doppler method for weak signals while both methods converge to the Cramér-Rao bound for strong signals. Finally, it is shown that in some cases of interest the proposed method inherently selects reliable observations while ignoring unreliable data.

Index Terms

Emitter location, Maximum likelihood estimation, Differential Doppler

* Corresponding author: Alon Amar, Tel: +97236408605, Fax: +97236407095, Email: amar@eng.tau.ac.il

§ Anthony J. Weiss, Tel: +97236407460, Fax: +97236407095, Email: ajw@eng.tau.ac.il

This research was supported by the Israel Science Foundation (grant No. 1232/04).

1. INTRODUCTION

A. Problem Description and Possible Applications

Passive position determination of a radiating emitter has been discussed in the literature since the Second World War. The position can be estimated by measuring one or more location-dependent signal parameters such as angle of arrival, time of arrival, received signal strength or Doppler frequency shift [1]-[4]. The idea of using the Doppler effect for localization found applications in radar, sonar, passive location systems (both for radio signals and acoustic signals), satellite positioning and navigation. To simplify the exhibition of our ideas we have chosen to address a specific application of localization using the Doppler effect. We focus on locating a stationary radio emitter by moving receivers. The motion induces frequency shift that is proportional to the signal frequency and to the radial velocity of each receiver towards (or away from) the emitter. It is assumed that the receiver location and velocity are known and therefore the emitter location can be estimated.

B. Related publications

One of the localization methods discussed in the literature is Differential Doppler (DD), also known as frequency difference of arrival. Differential-Doppler consists of measuring frequency differences between receivers since it eliminates the need to know the exact transmit frequency. The DD can be obtained by estimating the frequency at each receiver and then computing the difference [4, Section III] or by directly measuring the frequency difference using cross-correlation of the signals [5]-[7].

Differential Doppler has been proposed for locating moving emitter using stationary receivers in sonar [13],[14] and in artillery [15] applications. A similar problem of localizing a moving tone source has been discussed in [10]-[12] without employing DD. The contributions in [13],[14] essentially focus on aspects of frequency difference estimation rather than localization.

A system for localization of a stationary emitter can be implemented by at least a single platform carrying at least one receiver. Several platforms each carrying a single receiver are common. Becker [8] investigated the positioning error of a radar transmitting a pure, stable, unknown tone, based on multiple measurements of frequency and bearing, taken along a single platform trajectory. In [9] Becker extended his previous contribution by considering the drift and frequency hopping of the transmitted signal. Considering measurements collected by a single receiver, Fowler [17] investigated the accuracy of three-dimensional (3D) localization using terrain data. Levanon [16] discussed a DD location system based on two receivers on a single platform and compared its performance with an interferometer measurements. The Doppler effect has also been used for stationary emitters geolocation by satellites. The SARSAT/COSPAS [21] and the ARGOS [19] systems determine the emitter's position using a single satellite receiver. The satellite relays the observed signal to an earth station where the instance of zero Doppler shift is determined. Zero Doppler shift is associated with the point where the satellite is closest to the emitter, also known as the point of closest approach (PCA). The emitter's position is then determined from the PCA and the known satellite location and velocity. An error analysis of these systems has been presented by Levanon and Ben-Zaken [20]. An interesting and related application of localization based on the Doppler effect is demonstrated by the U.S. Navy TRANSIT system [25], [26]. The satellite is transmitting a tone observed by a relatively stationary receiver. The Doppler effect is used by the receiver to deduce its position. This system has been in use until 1991 for marine navigation and geodetic surveying. The localization of stationary emitter with multiple moving platforms has been discussed by Haworth *et al.* [22]. They presented a system for localizing satellite interference sources. The system is based on DD and time difference of arrival. Ho and Chan [23] considered the same system and provided an analytical solution for the source location. Later Pattison and Chou [24] examined the effect of

satellite position and velocity errors on the solution.

C. Objectives and contributions

All of the above mentioned approaches use two steps for localization. In the first step the Doppler frequency shifts, or their differences, are estimated without using the constraint that all estimates must correspond to the same emitter location and the same transmitted frequency. Only in the second step the location is estimated based on the results of the first step. Therefore, these methods are not guaranteed to yield optimal localization results.

The objective of this study is to propose a direct position determination method that optimally estimates the position of a stationary radio emitter by multiple moving platforms each equipped with a single receiver. The same principles that we employ here can be applied to other Doppler location configurations. Our method solves the location problem using the data collected by all receivers at all interception intervals using a single estimation step. The method can be applied to unknown signals and also to a-priori known signals such as beacon signals [21], training or synchronization sequences [27]. Based on the maximum likelihood estimation (MLE) principle the emitter location is determined as the position that is most likely to explain all the collected data. The proposed method requires only a single 3D search or 2D search if the emitter's plane is known. Simulations indicate that the proposed approach outperforms the two-step DD method under low signal to noise ratio (SNR) conditions, though both converge to the Cramér-Rao Lower Bound (CRLB) at high SNR. Also, in the presence of modeling errors the advocated method is superior. Compared to the two-step DD method, the proposed technique requires higher computation load. The new technique requires the transmission of the raw data to a central processor, as does the DD method, and therefore may require wider transmission bandwidth between the system units.

2. PROBLEM FORMULATION

Consider a stationary radio emitter and L moving receivers. The receivers are assumed to be synchronized in frequency and time. The emitter's position is denoted by the vector of coordinates $\mathbf{p}_0$. Each receiver intercepts the transmitted signal at K short intervals along its trajectory. Let $\mathbf{p}_{\ell,k}$ and $\mathbf{v}_{\ell,k}$ where $k = \{1, \ldots, K\}$ and $\ell = \{1, \ldots, L\}$ denote the position and velocity vectors of the ℓ-th receiver at the k-th interception interval, respectively. The complex signal observed by the ℓ-th receiver at the k-th interception interval at time t is

$$r_{\ell,k}(t) = b_{\ell,k} s_k(t) e^{j2\pi f_{\ell,k} t} + w_{\ell,k}(t), \quad 0 \leq t \leq T \tag{1}$$

where T is the observation time interval, $b_{\ell,k}$ is an unknown complex scalar representing the path attenuation at the k-th interception interval observed by the ℓ-th receiver, $s_k(t)$ is the observed signal envelope during the k-th interception interval, which may be known or unknown depending on the application, $w_{\ell,k}(t)$ is a wide sense stationary additive white zero mean complex Gaussian noise and finally $f_{\ell,k}$ is the frequency observed by the ℓ-th receiver during the k-th interception interval given by,

$$f_{\ell,k} \triangleq [f_c + \nu_k]\,[1 + \mu_{\ell,k}(\mathbf{p}_0)] \tag{2}$$

$$\mu_{\ell,k}(\mathbf{p}_0) \triangleq \frac{1}{c} \frac{\mathbf{v}_{\ell,k}^T [\mathbf{p}_0 - \mathbf{p}_{\ell,k}]}{\|\mathbf{p}_0 - \mathbf{p}_{\ell,k}\|} \tag{3}$$

where f_c is the nominal frequency of the transmitted signal, assumed known, ν_k is the unknown transmitted frequency shift due to the source instability, during the k-th interception interval and c is the signal's propagation speed.

Since $\mu_{\ell,k} \ll 1$ and $\nu_k \ll f_c$, Eq. (2) can be approximated as $f_{\ell,k} \cong \nu_k + f_c[1 + \mu_{\ell,k}(\mathbf{p}_0)]$ where the term $\nu_k \mu_{\ell,k}$, which is negligible with respect to (w.r.t.) all other terms, is omitted. Furthermore, as the nominal frequency, f_c, is known to the receivers, it is assumed that each

receiver performs a down conversion of the intercepted signal by the nominal frequency. Hence, after down conversion the frequency is $\bar{f}_{\ell,k} = f_{\ell,k} - f_c$ and Eq. (2) can be replaced by

$$\bar{f}_{\ell,k} \cong \nu_k + f_c \mu_{\ell,k}(\mathbf{p}_0) \tag{4}$$

The transmitted frequency is assumed to be constant during the interception interval, T. The down converted signal is sampled at times $t_n = nT_s$ where $n = \{0, \ldots, N-1\}$ and $T_s = T/(N-1)$. The signal at the k-th interception interval is given as $r_{\ell,k}[n] \stackrel{\Delta}{=} r_{\ell,k}(nT_s)$. Then Eq. (1) can be written in a vector form as

$$\mathbf{r}_{\ell,k} = b_{\ell,k}\mathbf{A}_{\ell,k}\mathbf{C}_k\mathbf{s}_k + \mathbf{w}_{\ell,k} \tag{5}$$

where

$$\mathbf{r}_{\ell,k} \stackrel{\Delta}{=} [r_{\ell,k}[0], \ldots, r_{\ell,k}[N-1]]^T \tag{6}$$

$$\mathbf{w}_{\ell,k} \stackrel{\Delta}{=} [w_{\ell,k}[0], \ldots, w_{\ell,k}[N-1]]^T \tag{7}$$

$$\mathbf{s}_k \stackrel{\Delta}{=} [s_k[0], \ldots, s_k[N-1]]^T \tag{8}$$

$$\mathbf{A}_{\ell,k} \stackrel{\Delta}{=} \text{diag}\left\{1, e^{j2\pi f_c \mu_{\ell,k} T_s}, \ldots, e^{j2\pi f_c \mu_{\ell,k}(N-1)T_s}\right\} \tag{9}$$

$$\mathbf{C}_k \stackrel{\Delta}{=} \text{diag}\left\{1, e^{j2\pi \nu_k T_s}, \ldots, e^{j2\pi \nu_k (N-1)T_s}\right\} \tag{10}$$

where diag$\{x_1, \ldots, x_n\}$ denotes a diagonal matrix with $\{x_1, \ldots, x_n\}$ on the main diagonal. Note in passing that these equations are accurate only if all the receivers are synchronized in frequency and in time. Moreover, the signal complex envelope $\mathbf{s}_k$ is the same at all spatially separated receivers provided that the signal bandwidth (rate of signal change) is small compared to the inverse of the propagation time between the receivers (i.e., $B < 1/\tau = c/d$. where τ, d are the maximal propagation time between the receivers and the the receivers spatial separation,

respectively.) This places a restriction on the receiver spatial separation for a given signal bandwidth.

It is to be noted that the matrix $\mathbf{A}_{\ell,k}$ is a function of the unknown emitter's position while the matrix $\mathbf{C}_k$ is a function of the unknown transmitted frequency. The noise vectors $\mathbf{w}_{\ell,k}$ are independent and normally distributed with zero mean and scaled identity covariance matrix, $\sigma_n^2\mathbf{I}$.

To summarize, the problem discussed here can be briefly stated as follows: Given the observation vectors $\{\mathbf{r}_{\ell,k}\}$ in Eq. (5), estimate the position of the emitter.

3. The Differential Doppler Localization Method

We describe the differential Doppler positioning approach in some detail. To simplify the exhibition we assume two receivers. Extensions to more receivers are straightforward. Denote by $\widehat{\Delta f}_k$ the estimated frequency difference, during the k-th interception interval, between the first receiver and the second receiver. As mentioned earlier, the frequency difference can be estimated by cross-correlation [5]-[7] of the two relevant signals or by estimating the frequencies at each receiver and then subtracting the estimated frequencies. Note that DD based on cross-correlation requires the transfer of raw data and therefore it is associated with higher transmission rates compared with methods that perform independent frequency measurement at each receiver and only have to transmit the result. Recently, a data compression technique has been proposed to reduce the transmission load [18].

The frequency difference is used in order to eliminate the unknown transmitted frequency offset ν_k. Using Eq. (4) the frequency difference associated with the k-th interception interval is given by

$$\widehat{\Delta f}_k = f_c \Delta m_k(\mathbf{p}_0) + \epsilon_k \tag{11}$$

where

$$\Delta m_k(\mathbf{p}_0) \stackrel{\Delta}{=} \mu_{1,k}(\mathbf{p}_0) - \mu_{2,k}(\mathbf{p}_0) \tag{12}$$

and ϵ_k is error reflecting the measurement errors and all other model errors. Using the least squares principle the position estimator is given by

$$\hat{\mathbf{p}}_0 = \underset{\mathbf{p}}{\operatorname{argmin}} \sum_{k=1}^{K} |\widehat{\Delta f}_k - f_c \Delta m_k(\mathbf{p})|^2 \tag{13}$$

The estimated emitter position is obtained by finding the minimum of the above cost function. Note that for accurate DD estimates the receivers should be frequency synchronized with high precision. Otherwise, the receivers frequency difference will affect the measurements. The position determination of the DD in (13) can be obtained by grid search or by iterative methods with a reasonable initial point.

4. Direct Position Determination Approach

Consider the observation vectors in Eq. (5). The information on the emitter's position is embedded in each of the matrices $\mathbf{A}_{\ell,k}$. This position is common to all observations at all interception intervals. Hence, we estimate the emitter position as the position that best explains all the data together. This is the main concept of the proposed direct position determination (DPD) approach.

Due to its excellent asymptotic properties (consistency and efficiency) we focus on the maximum likelihood estimator. The log-likelihood function of the observation vectors is given (up to an additive constant) by

$$L_1 = -\frac{1}{\sigma_n^2} \sum_{k=1}^{K} \sum_{\ell=1}^{L} \|\mathbf{r}_{\ell,k} - b_{\ell,k} \mathbf{A}_{\ell,k} \mathbf{C}_k \mathbf{s}_k\|^2 \tag{14}$$

The path attenuation scalars that maximizes Eq. (14) are given by

$$\begin{aligned}\hat{b}_{\ell,k} &= [(\mathbf{A}_{\ell,k}\mathbf{C}_k\mathbf{s}_k)^H\mathbf{A}_{\ell,k}\mathbf{C}_k\mathbf{s}_k]^{-1}(\mathbf{A}_{\ell,k}\mathbf{C}_k\mathbf{s}_k)^H\mathbf{r}_{\ell,k} \\ &= (\mathbf{A}_{\ell,k}\mathbf{C}_k\mathbf{s}_k)^H\mathbf{r}_{\ell,k} \qquad (15)\end{aligned}$$

where we assume, without loss of generality, that $\|\mathbf{s}_k\|^2 = 1$ and use the special structure of $\mathbf{A}_{\ell,k}$ and $\mathbf{C}_k$.

Substitution of Eq. (15) in Eq. (14) yields,

$$L_1 = -\frac{1}{\sigma_n^2}\left[\sum_{k=1}^{K}\sum_{\ell=1}^{L}\|\mathbf{r}_{\ell,k}\|^2 - |(\mathbf{A}_{\ell,k}\mathbf{C}_k\mathbf{s}_k)^H\mathbf{r}_{\ell,k}|^2\right] \qquad (16)$$

Since $\|\mathbf{r}_{\ell,k}\|^2$ is independent of the parameters, then instead of maximizing Eq. (16) we can now maximize the cost function L_2 given by

$$\begin{aligned}L_2 &= \sum_{k=1}^{K}\sum_{\ell=1}^{L}|(\mathbf{A}_{\ell,k}\mathbf{C}_k\mathbf{s}_k)^H\mathbf{r}_{\ell,k}|^2 \\ &= \sum_{k=1}^{K}\mathbf{u}_k^H\mathbf{Q}_k\mathbf{u}_k \qquad (17)\end{aligned}$$

where we defined the $N \times 1$ vector $\mathbf{u}_k$ as

$$\mathbf{u}_k \stackrel{\Delta}{=} \mathbf{C}_k\mathbf{s}_k \qquad (18)$$

and the $N \times N$ hermitian matrix $\mathbf{Q}_k$ as

$$\mathbf{Q}_k \stackrel{\Delta}{=} \mathbf{V}_k\mathbf{V}_k^H \qquad (19)$$

$$\mathbf{V}_k \stackrel{\Delta}{=} [\mathbf{A}_{1,k}^H\mathbf{r}_{1,k}, \cdots, \mathbf{A}_{L,k}^H\mathbf{r}_{L,k}] \qquad (20)$$

Two cases are considered now: unknown and a priori known transmitted signals. The first is a common assumption when there is no prior information on the signals. However, the second is

applicable to situations where the signals are a priori known to be training or synchronization sequences [27].

A. Unknown transmitted signals

When the transmitted signals are unknown, the cost function in Eq. (17) is maximized by maximizing each of the K quadratic forms w.r.t. $\mathbf{u}_k$, expressed in Eq. (18). Thus, the vector $\mathbf{u}_k$ should be selected as the eigenvector corresponding to the largest eigenvalue of the matrix $\mathbf{Q}_k$ [29, Section 1f.2, page 62].

Therefore, the cost function in Eq. (17) reduces to

$$L_{us} \;=\; \sum_{k=1}^{K} \lambda_{max}\{\mathbf{Q}_k\} \tag{21}$$

where the right hand side of Eq. (21) denotes the largest eigenvalue of the matrix $\mathbf{Q}_k$.

The dimension of the matrix $\mathbf{Q}_k$ is $N \times N$ and, therefore, it increases with the number of data samples. Determining the eigenvalues of $\mathbf{Q}_k$ can in turn result in high computation effort. Instead, it is known that given a matrix $\mathbf{X}$, the non-zero eigenvalues of $\mathbf{X}\mathbf{X}^H$ and $\mathbf{X}^H\mathbf{X}$ are identical [29, Section 1c.3, pp. 42-43]. Therefore, recalling the definition in Eq. (19), the $N \times N$ matrix $\mathbf{Q}_k$ in Eq. (21) can be replaced with the $L \times L$ matrix $\bar{\mathbf{Q}}_k$ given by

$$\bar{\mathbf{Q}}_k \stackrel{\Delta}{=} \mathbf{V}_k^H \mathbf{V}_k \tag{22}$$

This leads to a substantial reduction of the computation load whenever $L \ll N$.

The estimated emitter's position $\hat{\mathbf{p}}_0$ is now determined by a simple grid search. For any grid point, $\mathbf{p}$, in the position space, evaluate Eq. (21) with $\mathbf{Q}_k$ replaced by $\bar{\mathbf{Q}}_k$, and obtain

$$\bar{L}_{us}(\mathbf{p}) = \sum_{k=1}^{K} \lambda_{\max}\{\bar{\mathbf{Q}}_k\} \tag{23}$$

The estimated emitter's position is then given by

$$\hat{\mathbf{p}}_0 = \underset{\mathbf{p}}{\text{argmax}}\{\bar{L}_{us}(\mathbf{p})\} \tag{24}$$

An algorithm that uses the above equation to estimate the emitter position is usually more precise than a two-step procedure.

B. Known transmitted signals

Assuming that the transmitted signals are known, Eq. (17) can also be rewritten as,

$$L_2 \;=\; \sum_{k=1}^{K}\sum_{\ell=1}^{L} |\mathbf{r}_{\ell,k}^H \mathbf{A}_{\ell,k}\mathbf{S}_k\mathbf{c}_k|^2 \tag{25}$$

where we defined

$$\mathbf{S}_k \;\triangleq\; \text{diag}\{\mathbf{s}_k\} \tag{26}$$

$$\mathbf{c}_k \;\triangleq\; \text{diag}\{\mathbf{C}_k\} \tag{27}$$

In words, $\mathbf{S}_k$ is a diagonal matrix whose main diagonal is the vector $\mathbf{s}_k$ and $\mathbf{c}_k$ is a column vector consisting of the main diagonal elements of the matrix $\mathbf{C}_k$. Using Eq. (20) and Eq. (26), define the $L \times N$ matrix,

$$\mathbf{B}_k \triangleq \mathbf{V}_k^H \mathbf{S}_k \tag{28}$$

Now Eq. (25) can be simplified,

$$L_2 = \sum_{k=1}^{K} \|\mathbf{B}_k\mathbf{c}_k\|^2 \tag{29}$$

Recalling the definition of $\mathbf{c}_k$ in Eq. (27), and using Eq. (10), the last equation is a polynomial in $z \triangleq e^{j2\pi\nu_k T_s}$ and therefore for any given $\mathbf{B}_k$ the maximum of $\|\mathbf{B}_k\mathbf{c}_k\|^2$ w.r.t. ν_k can be obtained by the fast Fourier transform (FFT), as described in Appendix I.

The emitter position estimate, $\hat{\mathbf{p}}_0$, is now determined by a simple grid search. For each grid point, $\mathbf{p}$, in the position space, evaluate the K matrices $\{\mathbf{B}_k\}$ and use FFT to find ν_k that maximizes the expression $\|\mathbf{B}_k\mathbf{c}_k\|^2$. Define the cost function

$$L_{ks}(\mathbf{p}) = \sum_{k=1}^{K} \max_{\nu_k} \{\|\mathbf{B}_k\mathbf{c}_k\|^2\} \tag{30}$$

The estimated emitter's position is given by

$$\hat{\mathbf{p}}_0 = \underset{\mathbf{p}}{\text{argmax}}\{L_{ks}(\mathbf{p})\} \tag{31}$$

This concludes the derivation of the direct position determination algorithm for known signals.

5. Computation Load

In this section we assess the computation load of the differential Doppler and the proposed method assuming two receivers.

A. Differential Doppler

The MLE of the frequency difference, f, between two sequences $r_1[n], r_2[n]$ of length N, can be obtained from [7, Eq. (14)] by converting the equation to the time domain,

$$\hat{f} = \underset{f}{\text{argmax}} \left| \sum_{n=0}^{N-1} r_1[n] r_2^*[n] e^{j2\pi f n} \right| \tag{32}$$

In our case, $r_1[n]$ represents the sampled output of a receiver, and $r_2[n]$ may represent either the sampled output of a second receiver or samples of the known waveform.

An efficient implementation can be obtained by computing the FFT of $\{r_1[n]r_2^*[n]\}$. This involves N complex multiplications for obtaining $\{r_1[n]r_2^*[n]\}$ and $N\log_2 N$ multiplications for computing the FFT, and finally N complex multiplications for obtaining the squared absolute

value. Thus, along the track the total number of complex multiplications is $KN(2+\log_2 N) \approx KN\log_2 N$. This number will be doubled if the signals are known and frequency is estimated for each of the two receivers separately.

In the second step, the cost function in Eq. (13) is evaluated. For each point in the grid, $14K$ real multiplications (or $7K$ complex multiplications) are required. Thus, for N_g grid points, the total number of operations is dominated by, $7N_gK + KN\log_2 N$ if the signals are unknown and therefore cross-correlation is used, or $7N_gK + 2KN\log_2 N$ if the signals are known.

B. Proposed approach load

For known signals, the estimated position in our approach is determined by the maximum of Eq. (30) over all grid points. The number of multiplications required to evaluate $\mathbf{B}_k$ is $2NL$ since $\mathbf{A}_{k,\ell}$ and $\mathbf{S}_k$ are diagonal matrices. Since $\mathbf{B}_k$ is a $L \times N$ matrix, the number of multiplications required to evaluate the hermitian matrix $\mathbf{B}_k^H\mathbf{B}_k$ is approximately $0.5LN^2$. Therefore we need a total of $2NL + 0.5LN^2$ multiplications to evaluate $\mathbf{B}_k^H\mathbf{B}_k$. The scalar $\|\mathbf{B}_k\mathbf{c}_k\|^2$ is evaluated by FFT as described in Appendix I. The FFT requires approximately $N\log_2 N$ multiplications. The total number of operations, for N_g grid points, is therefore $N_gK(2NL + 0.5LN^2 + N\log_2 N) \cong 0.5N_gKLN^2$.

For unknown signals the evaluation of $\mathbf{V}_k$ in Eq. (19) requires NL multiplications and the evaluation of the hermitian matrix $\bar{\mathbf{Q}}_k$ requires approximately additional $0.5NL^2$ multiplications. Finding the eigenvalues in Eq. (23) requires L^3 multiplications. The total number of multiplications is $N_gK(L^3 + 0.5NL^2 + NL) \cong N_gKLN(0.5L + 1)$.

Thus, in most cases the proposed approach require considerably more computation than the DD, even if $L = 2$.

6. Simulation Results

In this section we examine the performance of the proposed method and compare it with the DD method and with the CRLB (detailed in Appendix II) using Monte-Carlo computer simulations. We focus on the position root mean square error (RMSE) defined by

$$\text{RMSE} = \sqrt{\frac{1}{N_{exp}} \sum_{i=1}^{N_{exp}} \|\hat{\mathbf{p}}_0(i) - \mathbf{p}_0\|^2} \tag{33}$$

where N_{exp} is the number of Monte-Carlo trials and $\hat{\mathbf{p}}_0(i)$ is the estimated emitter position at the i-th trial. To obtain statistical results we used $N_{exp} = 100$.

The simulated signal is a 10 Kilo-bits per second quadratic phase shift keying (QPSK) communication signal, sampled at 10 Kilo samples per second. Unless stated otherwise, we used 100 samples at each interception interval. The QPSK symbols were selected at random. The same signals were used for the known and unknown signal cases. The simulated nominal signal carrier frequency is $f_c = 0.1$ [GHz]. The propagation speed is assumed to be $c = 3 \cdot 10^8$ [m/sec].

The emitter's position is chosen at random within a square area of 10×10 [Km x Km]. The unknown transmitted frequency shifts, $\{\nu_k\}$, are selected at random from the interval $[-100, 100]$ [Hz]. The channel attenuation is selected at random from a normal distribution with mean one and standard deviation 0.1, and the channel phase is selected at random from a uniform distribution over $[-\pi, \pi)$. These parameters were then used for all trials.

We used maximum likelihood for estimating the frequency difference when simulating the DD approach for known and unknown signals, as described in Eq. (32). When the signals are known the frequency at each receiver is estimated by correlating the observed signal with the known expected signal. The frequency difference is then obtained by subtraction. When the signal is

unknown the observed signals at the receivers are cross-correlated one with the other to directly obtain the frequency difference. In both cases, the position is estimated as described in section 3.

Four different geometrical configurations are examined in this section. Fig. 1 summarizes the four cases. The solid lines show the receivers' trajectories where the triangles indicate the interception intervals. The emitter position is indicated by a small square. Unless stated otherwise, the receivers' speed is $v = 300$ [m/sec].

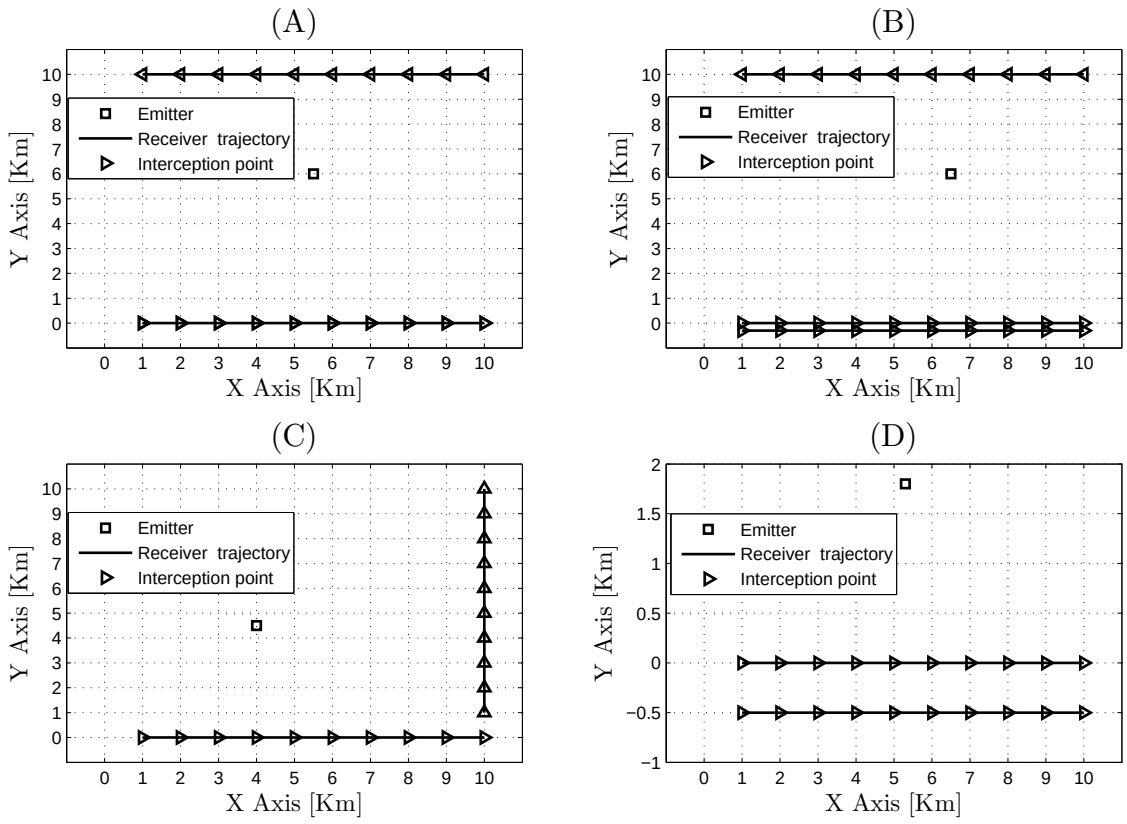

Fig. 1. Receivers' trajectories (solid lines), interception points (triangles) and emitter position (square) for 4 different cases.

Consider configurations A and B in Fig. 1. Configuration A describes two receivers ($L = 2$) one is moving leftwards and one is moving rightwards. Each receiver intercepts the signal at ten

different intervals ($K = 10$) along its trajectory. The first receiver intercepts the signal every one Kilometer starting at $[1, 0]$ [Km] and finishing at $[10, 0]$ [Km], and the second receiver intercepts the signal with the same spacing starting at $[10, 10]$ [Km] and finishing at $[1, 10]$ [Km]. A different case is illustrated in Figure 1-B. Here, three receivers ($L = 3$) are simulated. The trajectories, velocities, and the interception points of the first two receivers are the same as in Figure 1-A. The third receiver moves from $[1, -0.2]$ [Km] to $[10, -0.2]$ [Km] and intercepts the signal every 1 [Km]. The localization performance of the advocated method (DPD) is compared with the performance of the DD for known and unknown signals. The RMSE of position estimation versus SNR for known and unknown signals, and for two and three receivers are shown in Fig. 2. In all cases the DPD outperforms the DD at low SNR but at high SNR the methods are equivalent. (SNR is defined as the ratio of the average transmitted signal power to the average noise power.)

Next, DD and DPD are compared when the SNR is 20 [dB] for all receivers at all interception intervals except for the SNR of the second receiver at the last three interception intervals. The direction and speed of each receiver is as previously stated (Figure 1 subplot A). The SNR at the last three intervals is changed from 20 [dB] to -24 [dB] with a step of 2 [dB].

Fig. 3 shows the results. It can be seen that as the SNR at the last three intervals of the second receiver decreases, the performance of the two methods derogates. However, beyond a certain point, the performance of the DPD method improves in contrast with the conventional DD method. The DPD ignores the unreliable data and performs as if it does not exist.

In practical implementations of DD the outlier will probably be removed by a goodness-of-fit test (chi-square test). However, as demonstrated here the DPD works well without using such tests.

We also examine the position RMSE of both methods versus the number of samples N taken

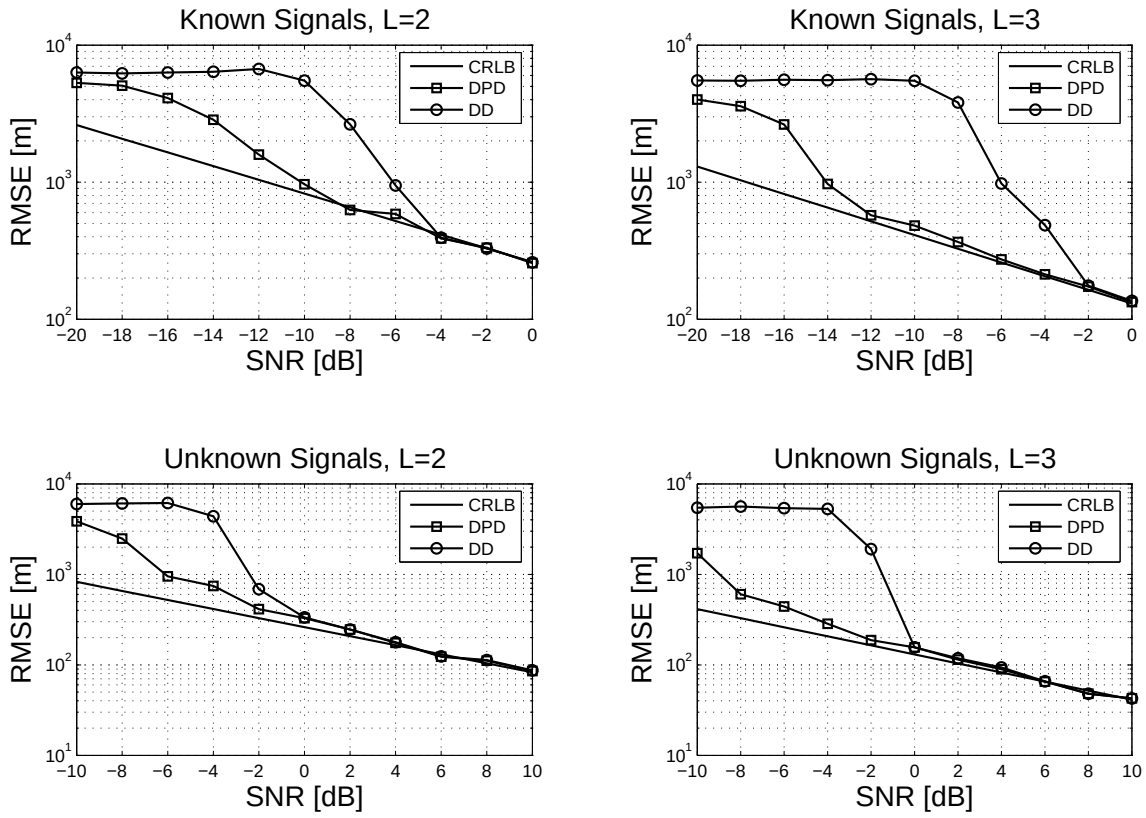

Fig. 2. RMSE of the DPD method, the DD method and the CRLB versus SNR with known and unknown transmitted signals, for two receivers (two left subplots) and three receivers (two right subplots).

in each interception interval. Consider configuration C in Fig. 1. The first receiver intercepts the signal from coordinate $[1, 0]$ [Km] to coordinate $[10, 0]$ [Km] every 1 [Km]. The second receiver intercepts the signal from coordinate $[10, 1]$ [Km] to coordinate $[10, 10]$ [Km] every 1 [Km]. We consider unknown transmitted signals. The SNR at each interception interval is SNR $= -5$[dB]. We examined the performances for $N = 100$ to $N = 500$ with a step of 20 samples. The position RMSE versus N for the DD and DPD methods compared with the CRLB is shown in Fig. 4. As can be seen for small number of samples (equivalent to low SNR), DPD outperforms the DD but as the number of samples increases both methods are equivalent. Note that as the N

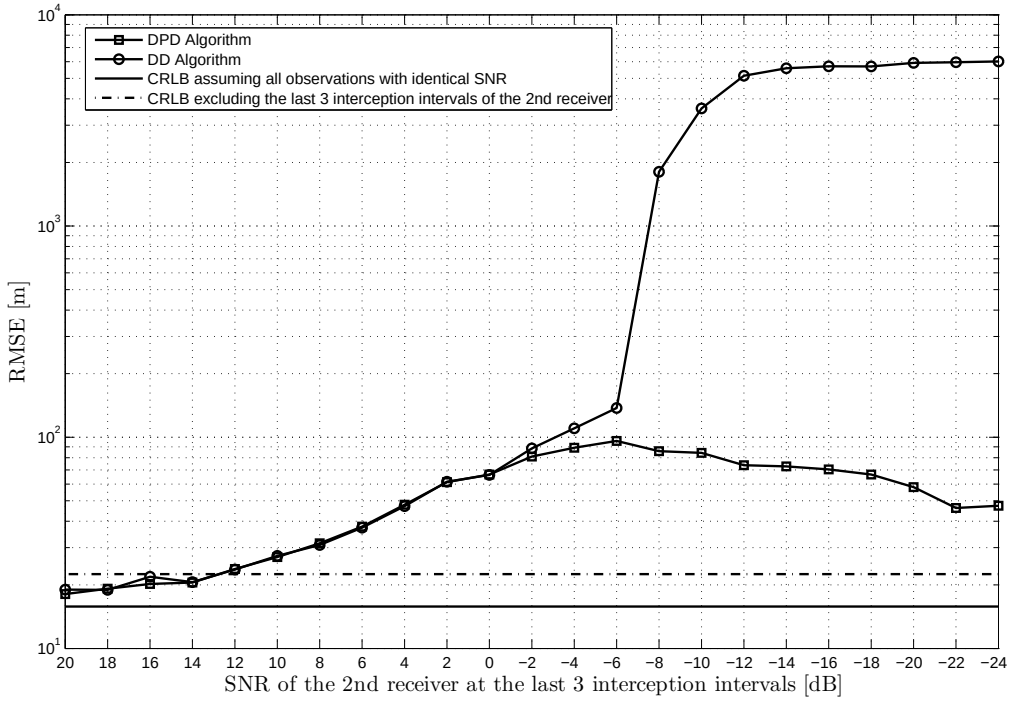

Fig. 3. RMSE of the DPD method and the DD method versus the SNR of the second receiver at the last three interception intervals.

increase the number of unknown also increases. This explains the gap between the RMSE and the CRLB.

We verified the assumption that the signal complex envelope $s_k(t)$ is the same at all spatially separated receivers. We consider configuration D in Fig. 1. The emitter's position is $[5, 5]$ [Km]. Two receivers ($L = 2$) are simulated. The first receiver intercepts the signal from coordinate $[1, 0]$ [Km] to coordinate $[10, 0]$ [Km] every 1 [Km]. The second receiver intercepts the signal from coordinate $[1, -y]$ [Km] to coordinate $[10, -y]$ [Km] every 1 [Km] where y is the distance between the receivers. This distance varies from 22 [Km] to 25 [Km] with a step of 0.2 [Km]. The SNR at each interception interval is SNR $= 10$ [dB] and the number of samples is $N = 100$. The position RMSE versus SNR for the DPD method compared with the CRLB is shown in Fig.

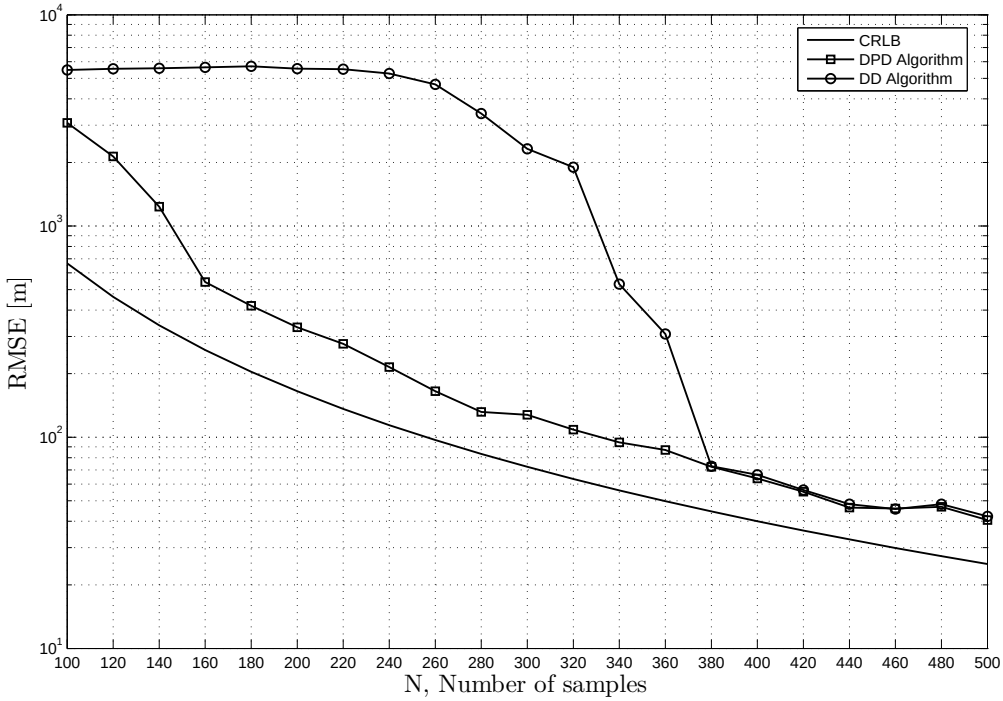

Fig. 4. RMSE of the DPD method, the DD method and the CRLB versus the number of samples N.

5. As can be seen up to $y \cong 25$ [Km] the RMSE of DPD is identical and close to the CRLB, and above this value the performance derogates. At this distance there is a change in a single symbol between the two receivers and therefore the complex envelopes are no more identical. Recall that we require that the signal's bandwidth is smaller than the inverse of the delay between the receivers. In our simulations the bandwidth is 10[KHz]. Thus the delay should be smaller than 0.1[msec]. In other words, the distance between the receivers should be smaller than 30[Km]. As can be seen this result closely agrees with the empirical result.

Finally, we plotted in Fig. 6 the DPD cost function for the configuration in Fig. 1. As is shown the cost function has a single peak at the position which is close to true emitter position. Due to the form of the cost function new iterative algorithms based on the DPD approach can

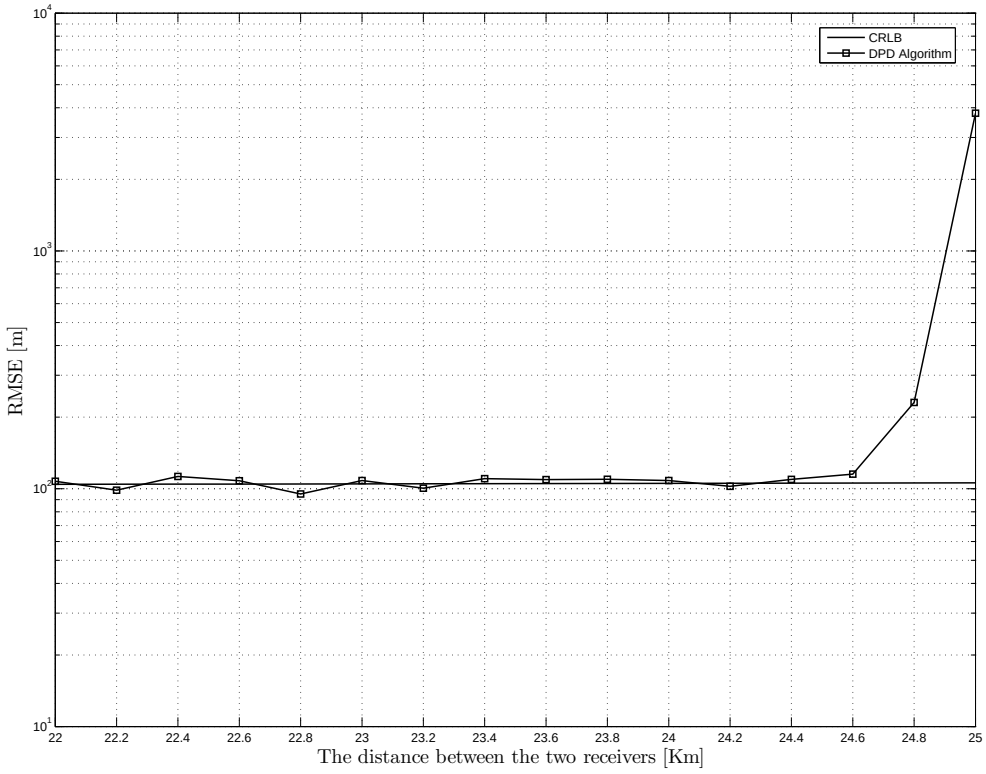

Fig. 5. RMSE of the DPD method, the DD method and the CRLB versus the distance between the two receivers.

be derived to reduce the current complexity.

7. CONCLUSIONS

Optimal location estimation of a stationary narrowband radio-frequency emitter, observed by moving receivers is discussed. The proposed method uses all the collected data together, in a single step, to estimate the emitter position by a grid search in the position space.

Changed from here:

Algorithms are derived for both known and unknown transmitted waveforms. It is demonstrated by several computer simulations that the proposed approach outperforms the conventional differential Doppler technique for different model parameters, such as the number of samples,

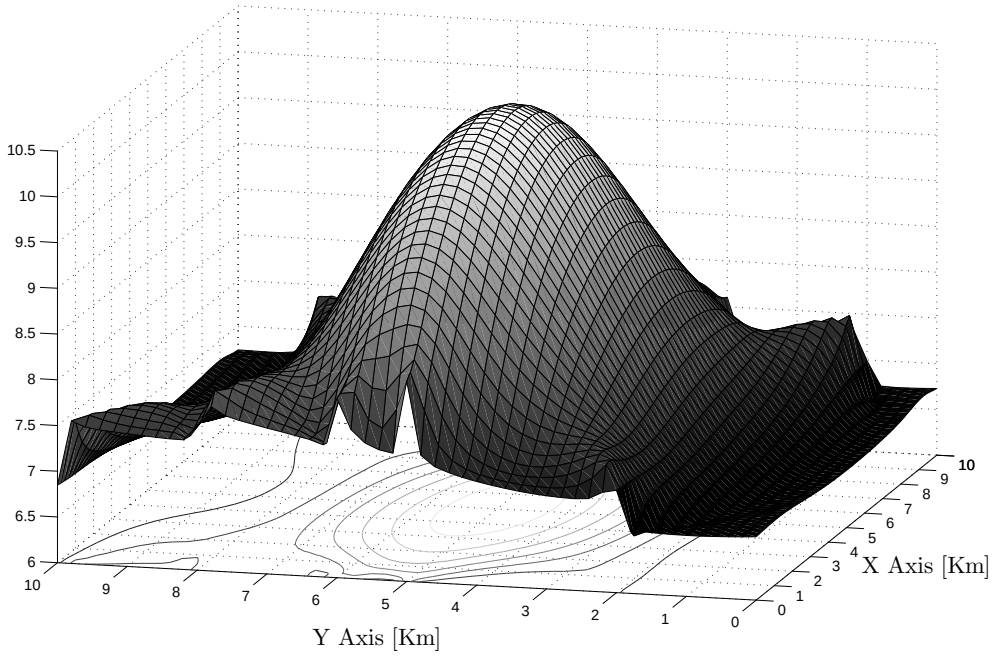

Fig. 6. The DPD cost function for the configuration in Figure 1.

the signal to noise ratio and the receivers configuration. However, The cost of performance improvement by employing the proposed direct position algorithms is the high complexity. Follow-on research will focus on the several aspects including: elaborating the proposed approach for localization of wideband signals; deriving iterative algorithms rather than grid-based to reduce complexity; and analyzing the performance of the proposed approach under model errors such frequency offsets or inaccuracies in the receivers' trajectories and velocities.

APPENDIX I
ESTIMATING ν_k VIA FFT

In this appendix we show how ν_k can be estimated using FFT. We are interested in finding the maximum of $\|\mathbf{B}_k\mathbf{c}_k\|^2 = \mathbf{c}_k^H\mathbf{B}_k^H\mathbf{B}_k\mathbf{c}_k$ w.r.t. ν_k where $\mathbf{c}_k = [1, z, \cdots z^{N-1}]^T$ and $z = e^{j2\pi\nu_k T_s}$.

Define the $N \times N$ matrix $\mathbf{G} \stackrel{\Delta}{=} \mathbf{B}_k^H \mathbf{B}_k$. Note that

$$\mathbf{c}_k^H \mathbf{B}_k^H \mathbf{B}_k \mathbf{c}_k = \sum_{i,j=1}^{N-1} \mathbf{G}[i,j] z^{i-j} = \sum_{m=-N+1}^{N-1} \alpha_m z^m \tag{34}$$

where $\mathbf{G}[i,j]$ is the (i,j)-th element of $\mathbf{G}$ and α_m is the sum of elements on the m-th diagonal of the $\mathbf{G}$. Since $\mathbf{G}$ is hermitian, $\alpha_m = \alpha_{-m}^*$. Let $\beta_0 = \alpha_0$ and $\beta_m = 2\alpha_m$ for $m = 1, \cdots, N-1$. We can rewrite Eq. (34) as

$$\mathbf{c}_k^H \mathbf{B}_k^H \mathbf{B}_k \mathbf{c}_k = \Re \left\{ \sum_{m=0}^{N-1} \beta_m^* z^{-m} \right\} \tag{35}$$

Thus, in order to find ν_k that maximizes $\|\mathbf{B}_k \mathbf{c}_k\|^2$, compute the FFT of the sequence $\{\beta_n^*\}_{n=0}^{N-1}$ and take the real part of the result. The FFT length should satisfy $M \geq N$. If the largest FFT coefficient is the m_0-th coefficient, then $\hat{\nu}_k = \frac{m_0}{MT_s}$ if $m_0 < M/2$, and $\hat{\nu}_k = -\frac{M-m_0}{MT_s}$ if $m_0 \geq M/2$. This concludes the appendix.

APPENDIX II
DERIVATION OF THE CRLB

In this appendix the CRLB is derived for the model in hand. The vector of transmitted frequencies is defined by

$$\boldsymbol{\nu} \stackrel{\Delta}{=} [\nu_1, \ldots, \nu_K]^T \tag{36}$$

the vector of path attenuations is defined by

$$\mathbf{b} \stackrel{\Delta}{=} [\mathbf{b}_1^T, \ldots, \mathbf{b}_K^T]^T \tag{37}$$

$$\mathbf{b}_k \stackrel{\Delta}{=} [b_{1,k}, \ldots, b_{L,k}]^T$$

and finally, the vector of observed signal envelopes is defined by

$$\mathbf{s} \stackrel{\Delta}{=} [\mathbf{s}_1^T, \ldots, \mathbf{s}_K^T]^T \tag{38}$$

We consider $\mathbf{p}_0$ as the vector of interest and $\boldsymbol{\nu}$, $\mathbf{b}$ and $\mathbf{s}$ as nuisance parameters. The parameter vector of the model in Eq. (5) is given by

$$\boldsymbol{\psi} \stackrel{\Delta}{=} \left[\mathbf{p}_0^T, \boldsymbol{\nu}^T, \bar{\mathbf{b}}^T, \tilde{\mathbf{b}}^T, \bar{\mathbf{s}}^T, \tilde{\mathbf{s}}^T\right]^T \tag{39}$$

where $\bar{\mathbf{x}}$ and $\tilde{\mathbf{x}}$ denotes the real and imaginary parts of the vector $\mathbf{x}$, respectively. We denote by

$$\breve{\mathbf{s}} \stackrel{\Delta}{=} [\bar{\mathbf{s}}^T, \tilde{\mathbf{s}}^T]^T \tag{40}$$

$$\breve{\mathbf{b}} \stackrel{\Delta}{=} [\bar{\mathbf{b}}^T, \tilde{\mathbf{b}}^T]^T \tag{41}$$

The CRLB bounds the mean square error of any unbiased estimator of $\boldsymbol{\psi}$, denoted by $\hat{\boldsymbol{\psi}}$ and is given by [28, Chapter 8]

$$\mathbf{E}\{(\hat{\boldsymbol{\psi}} - \boldsymbol{\psi})(\hat{\boldsymbol{\psi}} - \boldsymbol{\psi})^T\} \geq \mathbf{J}^{-1}(\boldsymbol{\psi}) \tag{42}$$

where $\mathbf{J}(\boldsymbol{\psi})$ is the Fisher information matrix (FIM) of the parameter vector $\boldsymbol{\psi}$. The FIM can be partitioned into blocks (sub-matrices),

$$\mathbf{J}(\boldsymbol{\psi}) \stackrel{\Delta}{=} \begin{bmatrix} \mathbf{J}_{\mathbf{p}_0\mathbf{p}_0} & \mathbf{J}_{\mathbf{p}_0\boldsymbol{\nu}} & \mathbf{J}_{\mathbf{p}_0\breve{\mathbf{b}}} & \mathbf{J}_{\mathbf{p}_0\breve{\mathbf{s}}} \\ \mathbf{J}_{\mathbf{p}_0\boldsymbol{\nu}}^T & \mathbf{J}_{\boldsymbol{\nu}\boldsymbol{\nu}} & \mathbf{J}_{\boldsymbol{\nu}\breve{\mathbf{b}}} & \mathbf{J}_{\boldsymbol{\nu}\breve{\mathbf{s}}} \\ \mathbf{J}_{\mathbf{p}_0\breve{\mathbf{b}}}^T & \mathbf{J}_{\boldsymbol{\nu}\breve{\mathbf{b}}}^T & \mathbf{J}_{\breve{\mathbf{b}}\breve{\mathbf{b}}} & \mathbf{J}_{\breve{\mathbf{b}}\breve{\mathbf{s}}} \\ \mathbf{J}_{\mathbf{p}_0\breve{\mathbf{s}}}^T & \mathbf{J}_{\boldsymbol{\nu}\breve{\mathbf{s}}}^T & \mathbf{J}_{\breve{\mathbf{b}}\breve{\mathbf{s}}}^T & \mathbf{J}_{\breve{\mathbf{s}}\breve{\mathbf{s}}} \end{bmatrix} \tag{43}$$

where $\mathbf{J}_{\mathbf{p}_0\mathbf{p}_0}$ is the FIM associated with the emitter's position $\mathbf{p}_0$, $\mathbf{J}_{\mathbf{p}_0\boldsymbol{\nu}}$ is the FIM associated with the position and frequencies. All other blocks are similarly defined. The CRLB of the emitter position is obtained by the upper left block of the FIM inverse.

The entries of the FIM in our case are given by [28, Section 8.23, Eq. (8.34)]

$$[\mathbf{J}(\boldsymbol{\psi})]_{n,m} \triangleq \frac{2}{\sigma_n^2} \sum_{k=1}^{K} \sum_{\ell=1}^{L} \Re \left\{ \frac{\partial (b_{\ell,k} \mathbf{A}_{\ell,k} \mathbf{C}_k \mathbf{s}_k)^H}{\partial \psi_n} \frac{\partial (b_{\ell,k} \mathbf{A}_{\ell,k} \mathbf{C}_k \mathbf{s}_k)}{\partial \psi_m} \right\} \tag{44}$$

Define,

$$\mathbf{S} \triangleq \text{Diag}\{\mathbf{I}_L \otimes \mathbf{s}_1, \cdots, \mathbf{I}_L \otimes \mathbf{s}_K\} \tag{45}$$

$$\mathbf{A} \triangleq \text{Diag}\{\mathbf{A}_{1,1}, \cdots, \mathbf{A}_{L,1}, \cdots, \mathbf{A}_{L,K}\} \tag{46}$$

$$\dot{\mathbf{A}} \triangleq \left[\frac{\partial \mathbf{A}}{\partial x}, \frac{\partial \mathbf{A}}{\partial y}\right] \tag{47}$$

$$\mathbf{C} \triangleq \text{Diag}\{\mathbf{I}_L \otimes \mathbf{C}_1, \cdots, \mathbf{I}_L \otimes \mathbf{C}_K\} \tag{48}$$

$$\dot{\mathbf{C}} \triangleq \text{Diag}\{\mathbf{I}_L \otimes \frac{\partial \mathbf{C}_1}{\partial \nu_1}, \cdots, \mathbf{I}_L \otimes \frac{\partial \mathbf{C}_K}{\partial \nu_K}\} \tag{49}$$

$$\mathbf{B} \triangleq \text{Diag}\{\mathbf{b}_1, \cdots, \mathbf{b}_K\} \tag{50}$$

where Diag$\{\mathbf{X}_1, \cdots, \mathbf{X}_M\}$ is a $NM \times RM$ block diagonal matrix with the $N \times R$ matrices $\mathbf{X}_m$, $m = 1, \ldots, M$, on the main diagonal.

It can be shown that the different blocks of the FIMs are

$$\mathbf{J}_{\mathbf{p}_0\mathbf{p}_0} = \frac{2}{\sigma_n^2}\Re\left\{(\mathbf{I}_2\otimes\mathbf{Sb})^H\dot{\mathbf{A}}^H\dot{\mathbf{A}}(\mathbf{I}_2\otimes\mathbf{Sb})\right\}$$

$$\mathbf{J}_{\mathbf{p}_0\boldsymbol{\nu}} = \frac{2}{\sigma_n^2}\Re\left\{(\mathbf{I}_2\otimes\mathbf{CSb})^H\dot{\mathbf{A}}^H\mathbf{A}\dot{\mathbf{C}}\mathbf{SB}\right\}$$

$$\mathbf{J}_{\mathbf{p}_0\check{\mathbf{b}}} = \frac{2}{\sigma_n^2}\left[\Re\left\{(\mathbf{I}_2\otimes\mathbf{Sb})^H\dot{\mathbf{A}}^H\mathbf{AS}\right\} - \Im\left\{(\mathbf{I}_2\otimes\mathbf{b})^H\mathbf{S}^H\dot{\mathbf{A}}^H\mathbf{AS}\right\}\right] \quad (51)$$

$$\mathbf{J}_{\mathbf{p}_0\check{\mathbf{s}}} = \frac{2}{\sigma_n^2}\left[\Re\left\{(\mathbf{I}_2\otimes\mathbf{Sb})^H\dot{\mathbf{A}}^H\mathbf{A}(\mathbf{B}\otimes\mathbf{I}_N)\right\} - \Im\left\{(\mathbf{I}_2\otimes\mathbf{b})^H\mathbf{S}^H\dot{\mathbf{A}}^H\mathbf{A}(\mathbf{B}\otimes\mathbf{I}_N)\right\}\right]$$

$$\mathbf{J}_{\boldsymbol{\nu}\boldsymbol{\nu}} = \frac{2}{\sigma_n^2}\Re\left\{\mathbf{B}^H\mathbf{S}^H\dot{\mathbf{C}}^H\dot{\mathbf{C}}\mathbf{SB}\right\}$$

$$\mathbf{J}_{\boldsymbol{\nu}\check{\mathbf{b}}} = \frac{2}{\sigma_n^2}\left[\Re\left\{\mathbf{B}^H\mathbf{S}^H\dot{\mathbf{C}}^H\mathbf{CS}\right\} - \Im\left\{\mathbf{B}^H\mathbf{S}^H\dot{\mathbf{C}}^H\mathbf{CS}\right\}\right] \quad (52)$$

$$\mathbf{J}_{\boldsymbol{\nu}\check{\mathbf{s}}} = \frac{2}{\sigma_n^2}\left[\Re\left\{\mathbf{B}^H\mathbf{S}^H\dot{\mathbf{C}}^H\mathbf{C}(\mathbf{B}\otimes\mathbf{I}_N)\right\} - \Im\left\{\mathbf{B}^H\mathbf{S}^H\dot{\mathbf{C}}^H\mathbf{C}(\mathbf{B}\otimes\mathbf{I}_N)\right\}\right]$$

$$\mathbf{J}_{\check{\mathbf{b}}\check{\mathbf{b}}} = \frac{2}{\sigma_n^2}\mathbf{I} \quad (53)$$

$$\mathbf{J}_{\check{\mathbf{b}}\check{\mathbf{s}}} = \frac{2}{\sigma_n^2}\begin{bmatrix}\Re\left\{\mathbf{S}^H(\mathbf{B}\otimes\mathbf{I}_N)\right\} & -\Im\left\{\mathbf{S}^H(\mathbf{B}\otimes\mathbf{I}_N)\right\}\\ \Im\left\{\mathbf{S}^H(\mathbf{B}\otimes\mathbf{I}_N)\right\} & \Re\left\{\mathbf{S}^H(\mathbf{B}\otimes\mathbf{I}_N)\right\}\end{bmatrix}$$

$$\mathbf{J}_{\check{\mathbf{s}}\check{\mathbf{s}}} = \frac{2}{\sigma_n^2}\begin{bmatrix}\mathbf{B}^H\mathbf{B} & \mathbf{0}\\ \mathbf{0} & \mathbf{B}^H\mathbf{B}\end{bmatrix}\otimes\mathbf{I}_N \quad (54)$$

If the signals are known the signal associated blocks should be removed. Recall that the signal at each interception interval is assumed to have a specified norm and its first element is real. Therefore, all row and columns associated with the real part and the imaginary part of the first signal element should be removed from $\mathbf{J}(\boldsymbol{\psi})$, if the signals are unknown. This concludes the

derivation.

REFERENCES

[1] G. Stansfield, "Statistical theory of DF fixing," *Journal IEE*, Vol. 94, Part 3A, No. 15, pp. 762-770, Dec. 1947.

[2] D. J. Torrieri, "Statistical theory of passive location systems," *IEEE Trans. on Aerospace and Electronic Systems*, Vol. AES-20, No. 2, pp. 183–198, Mar. 1984.

[3] M. Hata, and T. Nagatsu, "Mobile location using signal strength measurements in a cellular system," *IEEE Trans. on Vehicular Technology*, Vol. 29, No. 2, pp. 245–252, May 1980.

[4] P. C. Chestnut, "Emitter location accuracy using TDOA and differential Doppler," *IEEE Trans. on Aerospace and Electronic Systems*, Vol. AES-18, No. 2, pp. 214–218, Mar. 1982.

[5] C. H. Knapp, and G. C. Carter, "Estimation of time delay in the presence of source or receiver motion," *J. Acoust. Soc. Am.*, Vol. 61, No. 6, pp. 1545–1549, Jun. 1977.

[6] M. Wax, "The joint estimation of differential delay, Doppler, and phase," *IEEE Trans. on Information Theory*, Vol. IT-28, No. 5, pp. 817–820, Sep. 1982.

[7] S. Stein, "Differential delay/Doppler ML estimation with unknown signals," *IEEE Trans. on Signal Processing*, Vol. 41, No. 8, pp. 2717-2719, Aug. 1993.

[8] K. Becker, "An efficient method of passive emitter location," *IEEE Trans. on Aerospace and Electronic Systems*, Vol. 28, No. 4, pp. 1091–1104, Oct. 1992.

[9] K. Becker, "Passive localization of frequency-agile radars from angle and frequency measurements," *IEEE Trans. on Aerospace and Electronic Systems*, Vol. 35, No. 4, pp. 1129-1144, Oct. 1999.

[10] Y. T. Chan, and F. L. Jardine, "Target localization and tracking from Doppler shift measurments," *IEEE Journal of Oceanic Engineering*, Vol. 15, No. 3, pp. 251–257, Jul. 1990.

[11] Y. T. Chan, and J. J. Towers, "Passive localization from Doppler shifted frequency measurements," *IEEE Trans. on Signal Processing*, Vol. 40, No. 10, pp. 2594-2598, Oct. 1992.

[12] Y. T. Chan, and J. J. Towers, "Sequential localization of a radiating source by Doppler shifted frequency measurments," *IEEE Trans. on Aerospace and Electronic Systems*, Vol. 28, No. 4, pp. 1084–1090, Oct. 1992.

[13] P. M. Schultheiss, and E. Weinstein, "Estimation of differential Doppler shifts," *Journal Acoust. Soc. Am.*, Vol. 66, No. 5, pp. 1412-1419, Nov. 1979.

[14] E. Weinstein, "Measurement of the differential Doppler shift," *IEEE Trans. on Acoustics, Speech, and Signal Processing*, Vol. ASSP-30, No. 1, pp. 112–117, Feb. 1982.

[15] N. Levanon, and E. Weinstein, "Passive array tracking of a continuous wave transmitting projectile," *IEEE Trans. on Aerospace and Electronic Systems*, Vol. 16, No. 5, pp. 721–726, Sep. 1980.

[16] N. Levanon, "Interferometry against differential Doppler: performance comparison of two emitter location airborn systems," *IEE Proceedings*, Vol. 136, Pt. F, No. 2, pp. 70-74, Apr. 1989.

[17] M. L. Fowler, "Analysis of single platform passive emitter location with terrain data," *IEEE Trans. on Aerospace and Electronic Systems*, Vol. 37, No.2, pp. 495–507, Apr. 2001.

[18] M. L. Fowler, "Coarse quantization for data compression in coherent location systems," *IEEE Trans. on Aerospace and Electronic Systems*, Vol. 36, No. 4, pp. 1269–1278, Oct. 2000.

[19] J. L. Bessis, "Operational data collection and platform location by satellite," *Remote Sensing of the Environment*, Vol. 11, pp. 93–111, May 1981.

[20] N. Levanon, and M. Ben Zaken "Random error in ARGOS and SARSAT satellite positioning systems," *IEEE Trans. on Aerospace and Electronic Systems*, Vol. 21, No. 6, pp. 783–790, Nov. 1985.

[21] W. C. Scales, and R. Swanson "Air and sea rescue via satellite systems," *IEEE Spectrum*, Vol. 21, pp. 48–52, Mar. 1984.

[22] D. P. Haworth, N. G. Smith, R. Bardelli, and T. Clement, "Interference localization for the EUTELSAT satellites - the first European transmitter location system," *International Journal of Satellite Communications*, Vol. 15, No. 4, pp. 155–183, Sep. 1997.

[23] K. C. Ho, and Y. T. Chan, "Geolocation of a known altitude object from TDOA and FDOA measurements," *IEEE Trans. on Aerospace and Electronic Systems*, Vol. 33, No. 3, pp. 770–783, Jul. 1997.

[24] T. Pattison, and S. I. Chou, "Sensitivity analysis of dual satellite geolocation," *IEEE Trans. on Aerospace and Electronic Systems*, Vol. 36, No. 1, pp. 56–71, Jan. 2000.

[25] T. A. Stansell, "Positioning by satellites," appears in *Electronic Surveying and Navigation*, 2nd Ed., New York, NY: John Wiley & Sons, 1976, chapter 28, pp. 463-513.

[26] N. Levanon, "Theoretical bounds on random errors in satellite Doppler navigation," *IEEE Trans. on Aerospace and Electronic Systems*, Vol. 20, No. 6, pp. 810–816, Nov. 1984.

[27] J. Li, B. Halder, P. Stoica, and M. Viberg, "Computationally efficient angle estimation for signals with known waveforms," *IEEE Trans. on Signal Processing*, Vol. 43, No. 9, pp. 2154–2163, Sep. 1995.

[28] H. L. Van Trees, *Detection, Estimation, and Modulation Theory: Optimum Array Processing - Part IV*, New York, NY: John Wiley & Sons, 2002.

[29] C. R. Rao, *Linear Statistical Inference and Its Applications*, 2nd Ed., New York, NY: John Wiley & Sons, 2002.